Available online at www.sciencedirect.com
SCIENCE DIRECT
Superlattices and Microstructures 39 (2006) 348–357
Superlattices and Microstructures
www.elsevier.com/locate/superlattices

Expanding thermal plasma-deposited ZnO films: Substrate temperature influence on films properties. Film growth studies

I. Volintiru[a,*], M. Creatore[a], J.L. Linden[b], M.C.M. van de Sanden[a]

[a] *Eindhoven University of Technology, Department of Applied Physics, Eindhoven, The Netherlands*
[b] *TNO Science and Industry, Eindhoven, The Netherlands*

Available online 12 September 2005

Abstract

In this work, zinc oxide films were deposited using an argon-fed expanding thermal plasma with diethylzinc and oxygen admixed downstream. The substrate temperature influence on the films' electrical and structural properties has been investigated. An increase of crystallinity and surface roughness with increasing substrate temperature was found. The conductivity measurements indicated resistivity values as low as 4×10^{-3} Ω cm for the films deposited at 200 °C. For these films, in situ real-time spectroscopic ellipsometry was employed in order to investigate the film growth, i.e., the thickness evolution and the optical properties. Particular attention was paid to the evolution of the surface roughness, an important property in solar cell applications where a rough front electrode is needed for light trapping. Complementary ex situ diagnostics, such as atomic force microscopy and X-ray diffraction, were used to support the outcome of the ellipsometric investigation. The films deposited at 200 °C are found to be polycrystalline, with preferential (002) orientation and high surface roughness (up to 10% of the film thickness) at all investigated stages of growth.

Keywords: Zinc oxide; Expanding thermal plasma; Surface roughness; Spectroscopic ellipsometry

* Corresponding author. Tel.: +31 40 247 4882; fax: +31 40 245 6442.
E-mail address: i.m.volintiru@tue.nl (I. Volintiru).

0749-6036/$ - see front matter © 2005 Elsevier Ltd. All rights reserved.
doi:10.1016/j.spmi.2005.08.061

1. Introduction

Zinc oxide (ZnO) is one of the most studied transparent conductive oxides (TCOs) in the last decade due to its wide bandgap, large exciton binding energy, and piezoelectric character, useful in applications such as UV light emitters, solar cells, surface acoustic wave devices and organic light emitting diodes (OLEDs). High-conductivity n-type ZnO material with reproducible electro-optical and structural properties has already been obtained by many groups, including ours [1,2].

For the ZnO thin film deposition we use an Ar/O_2/diethylzinc expanding thermal plasma, which provides relatively high, not optimized deposition rates, up to 1 nm/s. The ZnO films show n-type conductivity (up to 250 Ω^{-1} cm^{-1}) and high transmittance in the visible range (>85%). The films also have a high native surface roughness of up to 10% of the film thickness, which is beneficial for light trapping in solar cell applications. The causes of this native roughness are not yet known. Previous studies [3,4] suggest that it could be due to the unintentionally incorporated water fragments (H_2O, OH, H). However, in various applications, films with different thickness/roughness are required: for example, while surface roughness is very beneficial in solar cells, a smooth surface is preferred in electronic devices. This makes the understanding of the roughness development during the ZnO film growth necessary. Gaining control of the film morphology would, therefore, allow one to address specific applications.

Spectroscopic ellipsometry (SE) has already been proven to be a very sensitive, non-intrusive tool in the real-time growth studies of, among others, hydrogenated amorphous silicon [5], microcrystalline silicon [6] or titanium nitride [7] films. However, to our knowledge, no in situ elipsometric investigation on ZnO morphology has been reported yet.

In this contribution we report on the effect of the substrate temperature on the ZnO surface roughness evolution, as well as on its electrical and structural properties. SE measurements will provide the ZnO film thickness and roughness evolution. Profilometry and Atomic Force Microscopy (AFM) will be used to support the outcome of the SE modeling, while X-ray Diffraction (XRD) will highlight the crystallinity development.

2. Experimental

The ZnO films were deposited using an expanding thermal plasma, generated in an argon-fed (840 sccm) high pressure (330 mbar) cascaded arc. The plasma expands supersonically in the low pressure (1.1 mbar) deposition chamber, where diethylzinc (2.5 g/h) and O_2 (50 sccm) are injected, via two separated injection rings, situated at 30 cm and 6.5 cm from the plasma source, respectively.

The films were deposited on p-type crystalline Si(100) (for ellipsometry measurements) and 400 nm thermal oxide (SiO_2)/c-Si(100) wafers (for the conductivity measurements). The substrate temperature was varied between 120 and 400 °C.

The real-time SE measurements were performed using a J.A. Woollam M2000U rotating compensator ellipsometer in the 250–1000 nm range. For data acquisition and processing, the WVASE software from Woollam was used. The ellipsometry measurements were performed both in situ (dynamic scans) and ex situ, after the deposition (static

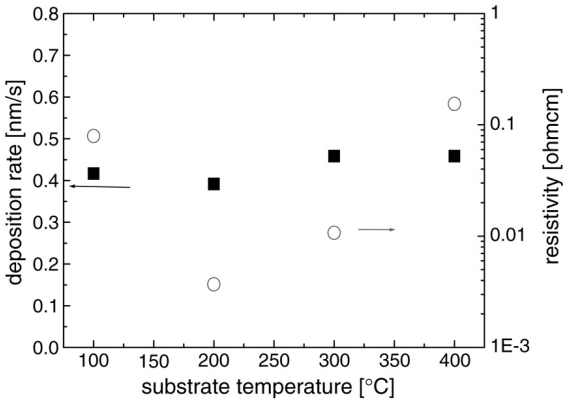

Fig. 1. ZnO film deposition rate and resistivity as a function of the substrate temperature.

scans), at an incidence angle of 61°. The spectral resolution was 1.6 nm. A full range scan was acquired every 2 s. The film thickness was measured using a Tencor P10 stylus profiler, with a tip diameter around 12.5 μm. For the sheet resistance measurements a Jandel universal four-point probe was used, with 0.5 mm diameter tungsten carbide tips and ∼1 mm spacing. The morphology measurements were performed with an NT-MDT Solver P47 atomic force microscope in the non-contact mode, using silicon cantilevers with curvatures below 10 nm. A Philips X-pert diffractometer with a CuK_{α} incident beam (1.54 Å), in normal configuration, was used for the XRD measurements.

3. Results

3.1. Substrate temperature influence on film properties

All films are n-type conductive, with resistivities between 4×10^{-3} and 0.2 Ω cm. The minimum resistivity is obtained for the films deposited at 200 °C. A similar behavior of the conductivity with substrate temperature has been also observed by Lin [8]. The deposition rate is ∼0.4 nm/s and it is, according to the profilometry measurements, unaffected by the substrate temperature (Fig. 1).

The surface morphology is strongly dependent on the substrate temperature, as shown by the AFM measurements (Fig. 2). The cause of the surface roughness in ZnO is not well known, many groups attributing this to H or OH groups present in the ZnO film, as already mentioned in the Introduction. While this is a possible explanation for the films deposited at low temperatures (<200 °C), on increasing the temperature it is generally observed that the density of the incorporated H/OH decreases [9]. At higher temperatures a smoother surface might be expected also due to an increase of surface mobility of the species and, consequently, of the concentration of the nucleation centers [10]. Therefore, for the ZnO deposited on thermal silica, another explanation for the increase of the surface roughness has to be found. The strain between the film and the substrate, increased by the high substrate temperature, could be the cause of the higher surface roughness at $T_{sub} > 200$ °C [11].

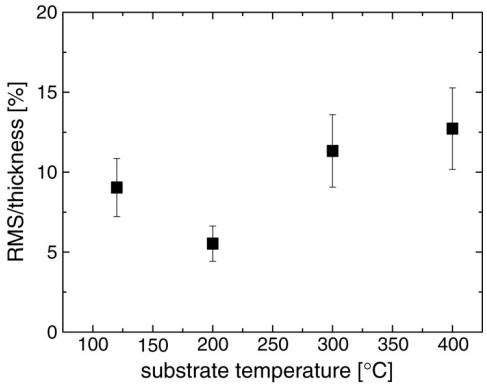

Fig. 2. Root-mean-square values normalized to the film thickness as a function of substrate temperature.

The XRD measurements showed polycrystalline films with (002) preferential orientation at all substrate temperatures (Fig. 3(a)). From the decrease of the (002) peak FWHM when increasing the substrate temperature (Fig. 3(b)) we can conclude that the crystallinity (grain size) is enhanced at higher temperatures, in agreement with other studies performed on similar material [8].

The decrease in conductivity (Fig. 1) could be explained by a constraint of the carrier mobility caused by the high roughness scale [12].

3.2. ZnO film growth monitoring

3.2.1. Spectroscopic ellipsometry

A few models for fitting the ex situ ellipsometry data have already been reported in the literature for ZnO [13–16]. We chose for our ZnO films to use a two-layer model, consisting of a bulk and a surface layer. For the optical constants of the bulk layer a Cauchy-like dispersion relation was used in the 450–1000 nm range:

$$\begin{aligned} n &= A + \frac{B}{\lambda^2} \\ k &= 0 \end{aligned} \tag{1}$$

where A and B are the Cauchy parameters. This model can be used for any material in its transparency domain.

The surface layer was modeled according to the commonly used Bruggeman Effective Medium Approximation (BEMA) [6], consisting of 50% bulk and 50% voids.

For the substrate we used tabulated values for the optical constants of the silicon at different temperatures, as well as for the native SiO_2 layer on top of it. The Mean Squared Error (MSE) was minimized by the WVASE program iteratively, according to the Marquardt–Levenberg fitting algorithm [17]. The film was assumed homogeneous on the whole area sampled by the ellipsometer and the SE spectra were modeled assuming abrupt flat interfaces between all layers, as well as uniformity in depth and isotropy of the optical constants of the substrate and the film.

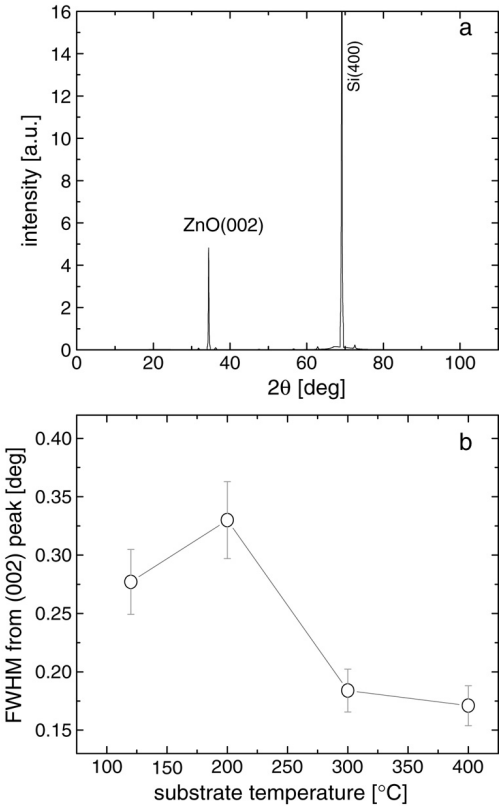

Fig. 3. (a) Typical XRD spectrum of a ZnO film; (b) the dependence of the (002) peak FWHM on the substrate temperature.

The spectroscopic ellipsometry analysis was performed on the ZnO films deposited at 200 °C, which showed the best conductivity and a reasonable low roughness ($<\lambda_{SE}/10$) for not causing extreme light depolarization.

A very good agreement between the model and the experimental data is obtained for film thicknesses below 200–250 nm. For thicker films, the roughness scale probably causes the light depolarization or/and a graded model to account for changes in the optical constants during growth may be more suitable. Therefore, we deposited ZnO films 250 nm thick on c-Si and recorded SE spectra during the deposition.

The optical constants were calculated both from the Cauchy model, presented above, and from point-by-point fits, i.e., using only the Kramer–Kronig relations. The values of both n and k (Fig. 4) are similar to those reported in the literature for undoped ZnO [18, 20–22].

We determined the optical constants from a Cauchy model fit of the final film and used these for the analysis of the bulk thickness/roughness development during growth. The (total) film thickness evolution, as well as the bulk thickness and the roughness evolution, is depicted in Fig. 5. The final thickness is confirmed by profilometry measurements.

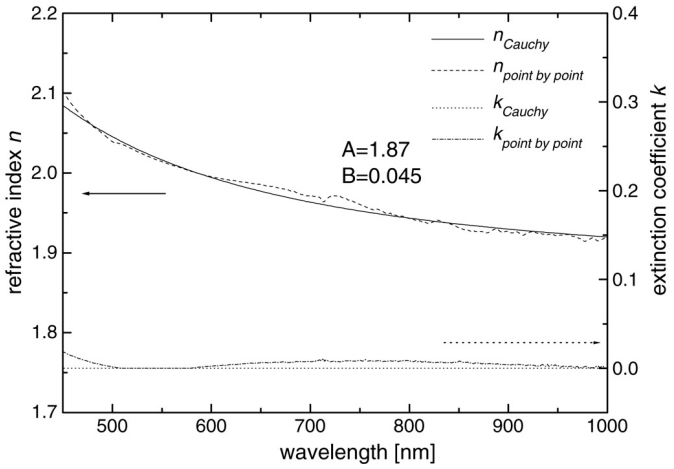

Fig. 4. Typical optical constants, as obtained from the Cauchy model (continuous lines) and the point-by-point fit (dashed curves) for a ZnO film of 250 nm.

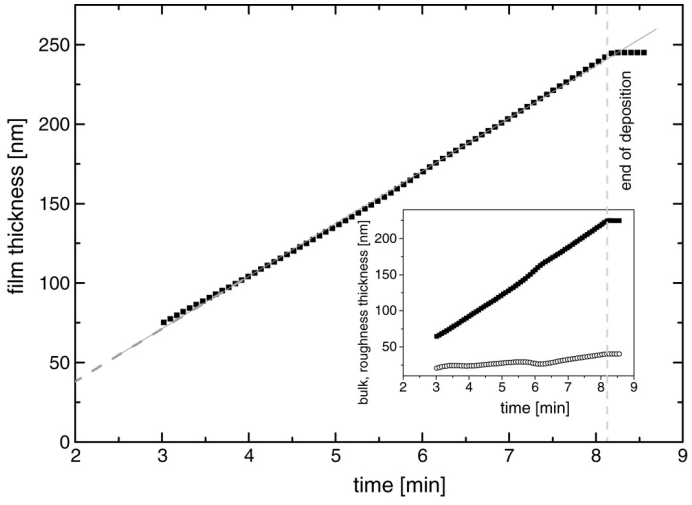

Fig. 5. The ZnO film thickness evolution during growth, as monitored by in situ SE; in the inset: the ZnO bulk and roughness layer thickness evolution during growth, as monitored by in situ SE.

Small fluctuations in the surface roughness and bulk evolution can be observed, probably due to the interference occurring in the ZnO layer and leading to very low intensity of the signal reaching the detector for specific film thicknesses [25]. The roughness and the bulk develop linearly above 50 nm, which indicates the same “bulk-like” material, with no island formation or transition from amorphous to crystalline phase.

Although the ellipsometric data were acquired from the beginning of the deposition, only film thicknesses above 70 nm are modeled. For thinner films it is very difficult

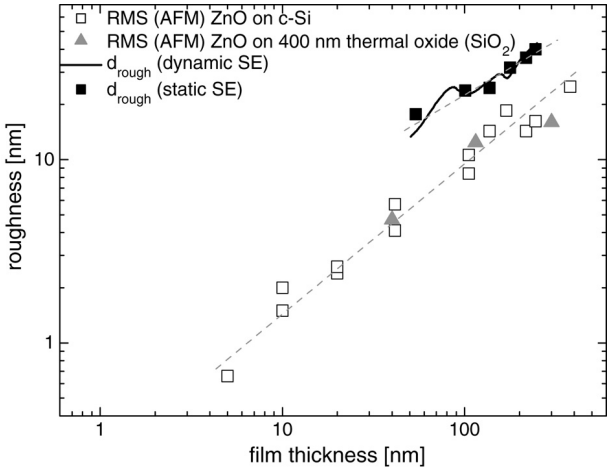

Fig. 6. The surface roughness evolution with film thickness, as measured by SE (static and dynamic) and by AFM.

to determine accurately both the film thickness and the refractive index using only the ellipsometry data. Complementary techniques need to be employed in order to have a good insight in the initial ZnO film growth.

Linear film thickness evolution is obtained for the whole modeled region (after 3 min of deposition) (Fig. 5). The delay observed in the thickness development (non-zero intercept with the time axis) can be an indication of the island formation and coalescence during the initial growth regime, similarly to what has been observed for other polycrystalline films [23,24].

3.2.2. Atomic force microscopy and X-ray diffraction

For validating the SE results, the surface roughness was also determined by AFM for films with different thicknesses. As our interest is mainly in the in situ real-time monitoring of the film growth, performed by SE, but not by AFM, a comparison between the film parameters obtained in situ during the deposition process and ex situ after air exposure needed to be investigated. In Fig. 6 it can be seen that the correspondence is reasonably good, showing that the ZnO films do not change significantly when exposed to the atmosphere. Also the use of two different substrates (c-Si and thermal SiO_2) does not influence the roughness evolution above 50 nm (Fig. 6).

Films with thicknesses between 50 and 250 nm were deposited and analyzed both by SE and AFM. Also thinner films (below 50 nm) were deposited and measured using AFM in order to provide a complete picture of the roughness evolution. The results are presented in Fig. 6.

The relation between the root mean square (RMS) value and the roughness layer thickness derived from the SE model is still under debate [6,19]. This occurs because both methods are influenced by many parameters, as mentioned before, but also due to the different nature of the roughness determined by the two techniques. However, the same

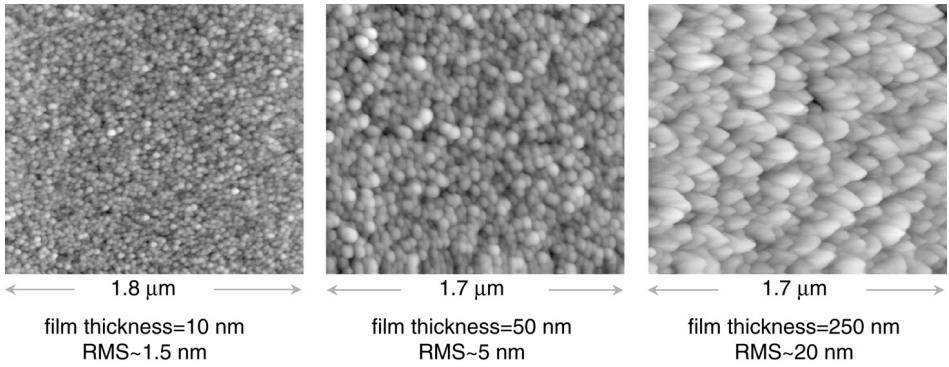

Fig. 7. AFM images of ZnO films with different film thicknesses.

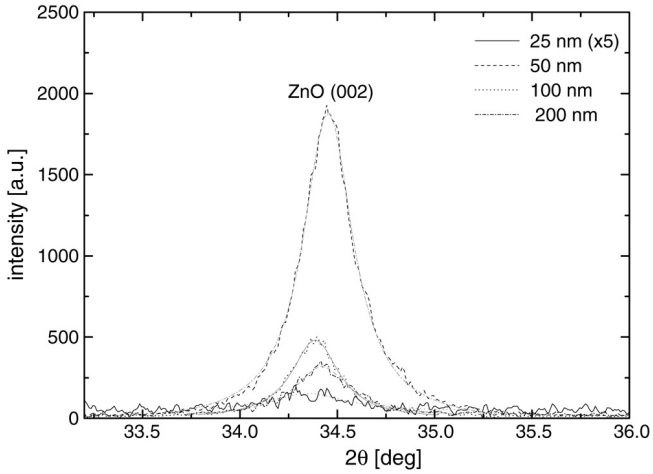

Fig. 8. The (002) peak region for ZnO films with thicknesses between 25 and 200 nm; because of the very low signal, the spectrum for the 10 nm film is not depicted here.

roughness evolution results from both measurements (Fig. 6), which makes the agreement between the two methods reasonable.

AFM images obtained for different film thickness are shown in Fig. 7. Besides the strong texture, which is clearly present at all investigated stages of the film growth, the increase of the correlation length during film growth (not shown here) also suggests a 3D grain development.

In order to see how the crystallinity develops during growth, XRD measurements were performed on the same films (Fig. 8). All scans showed preferential (002) orientation and no amorphous phase. This leads us to the conclusion that in our process the films grow crystalline in the (002) orientation already from 10 nm, and, if an amorphous-to-crystalline transition takes place (as expected in the initial stages for non-epitaxial growth),

it would occur below these film thicknesses. Also, very important for future applications, the roughness scale stays high (up to 10%) at all investigated stages of the deposition.

4. Conclusions

In this contribution, the influence of the substrate temperature on the ZnO film electrical, morphological and structural properties has been presented. We found an increase of crystallinity and surface roughness with increasing substrate temperature and optimum resistivity values (4×10^{-3} Ω cm) for the films deposited at 200 °C, as indicated by the conductivity measurements. For these films we also performed in situ studies using spectroscopic ellipsometry. Particular attention was paid to the surface roughness evolution, an important parameter in solar cell applications, where a rough front electrode is needed for light trapping.

A constant bulk and roughness development resulted from both SE and AFM measurements for films between 70 and 250 nm. Also a high surface roughness (up to 10% of the film thickness) at all investigated stages of growth is observed for the ZnO films deposited at 200 °C. The delay in the initial growth is probably caused by the formation and nucleation of the islands. This will be, however, a subject for future research. X-ray diffraction measurements indicated polycrystalline films, with preferential (002) orientation, no amorphous-to-crystalline transition occurring for films thicker than 10 nm.

Acknowledgments

The authors wish to thank J.P.J. van Jaarsveld for the AFM measurements and M.J.F. van de Sande, J.F.C. Jansen, and G. Kirchner for their technical assistance. This work was supported by the Netherlands Organization for Applied Scientific Research (TNO) and the Eindhoven University of Technology (TU/e) through the program for Sustainable Energy Technology (SET).

References

[1] R. Groenen, J. Löffler, P.M. Sommeling, J.L. Linden, E.A.G. Hamers, R.E.I. Schropp, M.C.M. van de Sanden, Thin Solid Films 392 (2001) 226.
[2] J. Springer, B. Rech, W. Reetz, J. Müller, M. Vanecek, Sol. Energy Mater. Sol. Cells 85 (2005) 1.
[3] T. Nakada, Y. Ohkubo, A. Kunioka, Japan. J. Appl. Phys. 30 (12A) (1991) 3344.
[4] S.J. Baik, J.H. Jang, C.H. Lee, W.Y. Cho, K.S. Lim, Appl. Phys. Lett. 70 (1997) 3516.
[5] N. Layadi, P. Roca i Cabarrocas, B. Drévillon, Phys. Rev. B 52 (1995) 5136.
[6] H. Fujiwara, M. Kondo, A. Matsuda, Phys. Rev. B 63 (2001) 115306-1.
[7] P. Patsalas, S. Logothetidis, Surf. Coat. Technol. 180–181 (2004) 421.
[8] S.S. Lin, J.L. Huang, D.F. Lii, Mater. Chem. Phys. 90 (2005) 22.
[9] M. Creatore, J.C. Cigal, G.M.W. Kroesen, M.C.M. van de Sanden, Thin Solid Films 484 (2005) 104–112.
[10] J.P.M. Hoefnagels, E. Langereis, W.M.M. Kessels, M.C.M. van de Sanden, IEEE Trans. Plasma Sci. 3 (2005) 234.
[11] N.E. Lee, D.G. Cahill, J.E. Greene, J. Appl. Phys. 80 (1996) 2199.
[12] L. Sagalowicz, G.R. Fox, J. Mater. Res. 14 (1999) 1876.
[13] S.J. Henley, M.N.R. Ashfold, D. Cherns, Surf. Coat. Technol. 177–178 (2004) 271.

[14] Z.F. Liu, F.K. Shan, Y.X. Li, B.C. Shin, Y.S. Yu, J. Cryst. Growth 259 (2003) 130.
[15] F.K. Shan, Y.S. Yu, J. Eur. Ceram. Soc. 24 (2004) 1869.
[16] Z.-C. Jin, I. Hamberg, C.G. Granqvist, J. Appl. Phys. 64 (1988) 5117.
[17] C.M. Herzinger, P.G. Snyder, B. Johs, J.A. Woollam, J. Appl. Phys. 77 (1995) 1715.
[18] H. Yoshikawa, S. Adachi, Japan. J. Appl. Phys. 36 (1997) 6237.
[19] P. Petrik, M. Fried, T. Lohner, R. Berger, L.P. Bíró, C. Schneider, J. Gyulai, H. Ryssel, Thin Solid Films 313–314 (1998) 259.
[20] X.W. Sun, H.S. Kwok, J. Appl. Phys. 86 (1999) 408.
[21] E. Dumont, B. Dugnoille, S. Bienfait, Thin Solid Films 353 (1999) 93.
[22] K. Postava, H. Sueki, M. Aoyama, T. Yamaguchi, Ch. Ino, Y. Igaseki, M. Horie, J. Appl. Phys. 87 (2000) 7820.
[23] H. Fujiwara, M. Kondo, A. Matsuda, J. Appl. Phys. 93 (2003) 2400.
[24] P. Patsalas, S. Logothetidis, J. Appl. Phys. 93 (2003) 989.
[25] P.J. van den Oever, M.C.M. van de Sanden, W.M.M. Kessels, Mater. Res. Soc. Symp. Proc. 808 (2004) A9.35.1.